

Combined action of the bound-electron nonlinearity and the tunnel-ionization current in low-order harmonic generation in noble gases

Usman Sapaev, Anton Husakou and Joachim Herrmann *

Max-Born-Institute for Nonlinear optics and Fast Spectroscopy, Max-Born-Str. 2a, Berlin D-12489, Germany

[*jherrman@mbi-berlin.de](mailto:jherrman@mbi-berlin.de)

Abstract: We study numerically low-order harmonic generation in noble gases pumped by intense femtosecond laser pulses in the tunneling ionization regime. We analyze the influence of the phase-mismatching on this process, caused by the generated plasma, and study in dependence on the pump intensity the origin of harmonic generation arising either from the bound-electron nonlinearity or the tunnel-ionization current. It is shown that in argon the optimum pump intensity of about 100 TW/cm^2 leads to the maximum efficiency, where the main contribution to low-order harmonics originates from the bound-electron third and fifth order susceptibilities, while for intensities higher than 300 TW/cm^2 the tunnel-ionization current plays the dominant role. Besides, we predict that VUV pulses at 133 nm can be generated with relatively high efficiency of about 1.5×10^{-3} by 400 nm pump pulses.

© 2019 Optical Society of America

OCIS codes: (190.0190) Nonlinear optics; (190.2620) Harmonic generation and mixing; (190.7110) Ultrafast nonlinear optics.

References and links

1. I. V. Hertel and W. Radloff, "Ultrafast dynamics in isolated molecules and molecular clusters," *Rep. Prog. Phys.* **69**, 1897–2003 (2006).
2. S. Backus, J. Peatross, Z. Zeek, A. Rundquist, G. Taft, M. M. Murnane, and H. C. Kapteyn, "16-fs, 1-J ultraviolet pulses generated by third-harmonic conversion in air," *Opt. Lett.* **21**, 665–667 (1997).
3. S. A. Trushin, K. Kosma, W. Fuß, and W. E. Schmid, "Sub-10-fs supercontinuum radiation generated by filamentation of few-cycle 800 nm pulses in argon," *Opt. Lett.* **32**, 2432–2434 (2007).
4. K. Kosma, S. A. Trushin, W. E. Schmid, and W. Fuß, "Vacuum ultraviolet pulses of 11 fs from fifth-harmonic generation of a Ti:sapphire laser," *Opt. Lett.* **33**, 723–725 (2008).
5. C. G. Durfee, S. B. Margaret, M. Murnane, and H. C. Kapteyn, "Ultrabroadband phase-matched optical parametric generation in the ultraviolet by use of guided waves," *Opt. Lett.* **22**, 1565–1567 (1997).
6. P. Tzankov, O. Steinkellner, J. Zheng, M. Mero, W. Freyer, A. Husakou, I. Babushkin, J. Herrmann, and F. Noack, "High-power fifth-harmonic generation of femtosecond pulses in the vacuum ultraviolet using a Ti:sapphire laser," *Opt. Express* **15**, 6389–6395 (2007), <http://www.opticsinfobase.org/abstract.cfm?URI=oe-15-10-6389>.
7. I. V. Babushkin and J. Herrmann, "High energy sub-10 fs pulse generation in vacuum ultraviolet using chirped four wave mixing in hollow waveguides," *Opt. Express* **16**, 17774–17779 (2008), <http://www.opticsinfobase.org/oe/abstract.cfm?uri=oe-16-22-17774>.
8. A. Paul, R. A. Bartels, R. Tobey, H. Green, S. Weiman, I. P. Christov, M. M. Murnane, H. C. Kapteyn, and S. Backus, "Quasi-phase-matched generation of coherent extreme-ultraviolet light," *Nature (London)* **421**, 51–54 (2003).

9. U. K. Sapaev, I. V. Babushkin and J. Herrmann, "Quasi-phase-matching for third harmonic generation in noble gases employing ultrasound," *Opt. Express* **20**, 22753–22762 (2012), <http://www.opticsinfobase.org/oe/abstract.cfm?uri=oe-20-20-22753>.
10. M. Ghotbi, M. Beutler, and F. Noack, "Generation of 2.5 μ J vacuum ultraviolet pulses with sub-50 fs duration by noncollinear four-wave mixing in argon," *Opt. Lett.* **35**, 3492–3494 (2010).
11. M. Ghotbi, P. Trabs, M. Beutler, and F. Noack, "Generation of tunable sub-45 femtosecond pulses by noncollinear four-wave mixing," *Opt. Lett.* **38**, 486–488 (2013).
12. C. Bree, A. Demircan, and G. Steinmeyer, "Multiple-harmonic conversion of 1064 nm radiation in rare gases," *Phys. Rev. Lett.* **106**, 183902 (2011).
13. F. Krausz and M. Ivanov, "Attosecond physics," *Rev. Mod. Phys.* **81**, 163–234 (2009).
14. F. Brunel, "Harmonic generation due to plasma effects in a gas undergoing multiphoton ionization in the high-intensity limit," *J. Opt. Soc. Am. B* **7**, 521–526 (1990).
15. N. H. Burnett, C. Kan, and P. B. Corkum, "Ellipticity and polarization effects in harmonic generation in ionizing neon," *Phys. Rev. A* **51**, 3418–3420 (1995).
16. E. V. Vanin, A. V. Kim, A. M. Sergeev, M. C. Downer, "Excitation of ultrashort bursts of harmonics of the radiation during ionization of a gas by an intense light pulse," *Sov. Phys. JETP Lett.* **58**, 900–906 (1993).
17. E. E. Serebryannikov, A. J. Verhoef, A. Mitrofanov, A. Baltuška, and A. M. Zheltikov, "Ellipticity and polarization effects in harmonic generation in ionizing neon," *Phys. Rev. A* **80**, 053809 (2009).
18. K. Y. Kim, J. H. Glowina, A. J. Taylor, and G. Rodriguez, "Terahertz emission from ultrafast ionizing air in symmetry-broken laser fields," *Opt. Express* **15**, 4577–4584 (2007), <http://www.opticsinfobase.org/oe/abstract.cfm?uri=oe-15-8-4577>.
19. I. Babushkin, W. Kuehn, C. Köhler, S. Skupin, L. Bergé, K. Reimann, M. Woerner, J. Herrmann, and T. Elsaesser, "Ultrafast spatiotemporal dynamics of terahertz generation by ionizing two-color femtosecond pulses in gases," *Phys. Rev. Lett.* **105**, 053903 (2010).
20. I. Babushkin, S. Skupin, A. Husakou, C. Köhler, E. Cabrera-Granado, L. Bergé, and J. Herrmann, "Tailoring terahertz radiation by controlling tunnel photoionization events in gases," *New J. Phys.* **13**, 123029 (2011).
21. C. W. Siders, G. Rodriguez, J. L. W. Siders, F. G. Omenetto, and A. J. Taylor, "Measurement of ultrafast ionization dynamics of gases by multipulse interferometric frequency-resolved optical gating," *Phys. Rev. Lett.* **87**, 263002 (2001).
22. J. Verhoef, A. V. Mitrofanov, E. E. Serebryannikov, D. V. Kartashov, A. M. Zheltikov, and A. Baltuška, "Optical Detection of Tunneling Ionization," *Phys. Rev. Lett.* **104**, 163904 (2010).
23. C. W. Siders, N. C. Turner, M. C. Downer, A. Babine, A. Stepanov, and A. M. Sergeev, "Blue-shifted third-harmonic generation and correlated self-guiding during ultrafast barrier suppression ionization of subatmospheric density noble gases," *J. Opt. Soc. Am. B* **13**, 330–335 (1996).
24. J. F. Ward and G. H. C. New, "Optical third harmonic generation in gases by a focused laser beam," *Phys. Rev.* **185**, 57–72 (1969).
25. G. C. Bjorklund, "Effects of focusing on third-order nonlinear processes in isotropic media," *IEEE J. Quantum Electron.* **11**, 287–296 (1975).
26. A. V. Husakou and J. Herrmann, "Supercontinuum generation of higher-order solitons by fission in photonic crystal fibers," *Phys. Rev. Lett.* **87**, 203901 (2001).
27. M. V. Ammosov, N. Delone, and V. P. Krainov, "Tunnel ionization of complex atoms and of atomic ions in an alternating electromagnetic field," *Sov. Phys. JETP* **91**, 2008–2013 (1986).
28. Z. Chang, *Fundamentals of Attosecond Optics* (Taylor and Francis Group, 2011).
29. Z. Song, Y. Qin, G. Zhang, S. Cao, D. Pang, L. Chai, Q. Wanga, Z. Wangb, and Z. Zhang, "Femtosecond pulse propagation in temperature controlled gas-filled hollow fiber," *Opt. Commun.* **281**, 4109–4113 (2008).
30. C. Bree, "Nonlinear optics in the filamentation regime," Ph.D. Dissertation (2012), <http://edoc.hu-berlin.de/dissertationen/bree-carsten-2011-09-21/PDF/bree.pdf>.
31. V. Loriot, E. Hertz, O. Faucher, and B. Lavorel, "Measurement of high order Kerr refractive index of major air components," *Opt. Express* **17**, 13429–13434 (2009), <http://www.opticsinfobase.org/oe/abstract.cfm?uri=oe-17-16-13429>.
32. J. Ni, J. Yao, B. Zeng, W. Chu, G. Li, H. Zhang, C. Jing, S. L. Chin, Y. Cheng and Z. Xu, "Comparative investigation of third- and fifth-harmonic generation in atomic and molecular gases driven by midinfrared ultrafast laser pulses," *Phys. Rev. A* **84**, 063846 (2011).
33. W. F. Chan, G. Cooper, X. Guo, G. R. Burton, and C. E. Brion, "Absolute optical oscillator strengths for the electronic excitation of atoms at high resolution. III. The photoabsorption of argon, krypton, and xenon," *Phys. Rev. A* **46**, 149–171 (1992).

1. Introduction

Low-order harmonic generation (LOHG) in gases pumped by ultrashort near-IR laser pulses is an important technique to generate ultraviolet (UV) and vacuum ultraviolet (VUV) femtosec-

ond pulses for a wide variety of applications, in particular, for time-resolved spectroscopy of many molecules, clusters or biological specimens and for material characterization [1]. The use of noble gases as nonlinear medium instead of solid-state crystals is a preferable way to avoid strong dispersion, bandwidth limitations, low damage thresholds and strong absorption below 200 nm. In particular, by using different gases UV and VUV pulses with a duration down to 11 fs have been generated by third [2,3] and fifth harmonic [4] conversion. Similar to other nonlinear frequency conversion processes, the efficiency of LOHG in gases is usually relatively low in practice. This is mainly caused by two factors: first, low conversion results from relatively small values of the third (and higher) order susceptibilities compared to crystalline media. A second problem is the realization of phase matching, which can be partially solved for various frequency transformation processes, e.g., by using the anomalous dispersion of hollow-core fibers [5–7], modulated hollow-core waveguides [8], a modulated third order nonlinearity by ultrasound [9] or by noncollinear four-wave mixing [10, 11].

In the intensity range below the ionization threshold the efficiency of frequency transformation increases with increasing pump intensity. However, as soon as the intensity rises above the ionization threshold, different additional processes play a role leading to a more complex dynamics. On the one hand the effective third-order nonlinearity decreases, since $\chi^{(3)}$ of an ionized gas is lower than $\chi^{(3)}$ of a corresponding neutral gas [12]. On the other hand harmonics of the fundamental frequency emerge due to the ionization of the atoms and the interaction of the freed electrons with the intense pump field. The majority of studies of harmonic generation have been performed for relatively high orders of harmonics much in excess of the ionization potential which is well described by the three-step process of ionization, acceleration in the continuum and recombination with the parent ion (see e.g. [13]). Much less studied is an additional, physically different, mechanism of optical harmonic generation. In the regime of tunneling ionization the density of ionized electrons shows extremely fast, nearly stepwise increases at every half-cycle of the laser field. This stepwise modulation of the tunnel ionization current induces optical harmonic generation [14], which arises in the first stage of ionization and not in the final recombination stage in the three-step model. As shown in [15], the emission of the lowest harmonics up to about 9 are accounted for with the tunnel ionization current while higher orders are attributed with the recombination process. Further theoretical studies of this process has been published in [16, 17]. Note that the generation of THz pulses by two-color femtosecond pulses is also intrinsically connected to the optically induced step-wise increase of the plasma density due to tunneling ionization [18–20].

To date only few direct experimental observations of harmonic generation or frequency mixing due to the modulation of the tunnel ionization current has been reported [21, 22]. On the other hand the generation of third harmonics with efficiencies up to the range of 10^{-3} in a noble gas with pump intensities significantly larger than necessary for ionization has been reported in [2, 23]. Detections of this type of nonlinear response in the regime with intensities above the ionization threshold requires better understanding of the complex dynamics and insight into the competition of harmonic generation originating from atomic or ionic susceptibilities of bound states and the tunneling ionization current. The present paper is devoted to a theoretical study of this issue. Since here only low orders up to 7 are considered we neglect the recombination process and consider only the first stage of ionization. At least, up to our knowledge the combined occurrence of the two mechanisms by the bound-electron third (and higher) order nonlinearity and the tunnel-ionization current were not studied before.

2. Fundamentals

Third harmonic generation (THG) in gases by focused beams for pump intensities below the ionization threshold has been studied theoretically already four decades ago [24, 25]. In the

regime of tunneling ionization besides the nonlinearity due to bound electron states additional processes come into play which has to be accounted for. In particular, the sub-cycle temporal dynamic of the laser field plays an essential role in the ionization process. Therefore, in the theoretical description the slowly-varying envelope approximation requires the solution of a complicated, strongly coupled system of partial differential equations and would result in increased numerical errors due to relatively short (down to 8 fs) durations of harmonic pulses. Since backward propagating field components are small we can use the unidirectional pulse propagation equation for the description of pulse propagation [26]. As will be seen later the effective propagation length is much smaller than the Rayleigh length, therefore we can neglect the diffraction term. Correspondingly the following basic equation for the electric field of linear polarized pulses will be used:

$$\partial_z \hat{E}(\omega) = ik(\omega)\hat{E}(\omega) + i\frac{\mu_o\omega^2}{2k(\omega)}\hat{P}_{NL}(\omega) \quad (1)$$

Here $\hat{E}(\omega)$ is the Fourier transform of the electric field $E(t)$; $k(\omega) = cn(\omega)/\omega$ is the frequency-dependent wavenumber, ω is the angular frequency, c is the speed of light and $n(\omega)$ is the frequency-dependent refractive index of the chosen gas; μ_o is the vacuum permeability. The first term on the right-hand side of Eq. (1) describes linear dispersion of the gas. The nonlinear polarization is $\hat{P}_{NL}(\omega) = \hat{P}_{Bound}(\omega) + i\hat{J}_e(\omega)/\omega + i\hat{J}_{Loss}(\omega)/\omega$ with $\hat{P}_{Bound}(\omega)$ being the nonlinear polarization caused by the bound electron states, $\hat{J}_e(\omega)$ being the electron current and $\hat{J}_{Loss}(\omega)$ being the loss term due to photon absorption during ionization. The plasma dynamics is described by the free electron density $\rho(t)$, which can be calculated by:

$$\partial_t \rho(t) = W_{ST}(t)(\rho_{at} - \rho(t)) \quad (2)$$

where ρ_{at} is the neutral atomic density; $W_{ST}(t)$ is the quasistatic tunneling ionization rate for hydrogenlike atoms [27] $W_{ST}(t) = 4\omega_a(r_h)^{2.5}(|E_a|/E(t))\exp(-2r^{1.5}|E_a|/3E(t))$, where $E_a = m_e^2 q^5 / (4\pi\epsilon_o)^3 \hbar^4$, $\omega_a = m_e q^4 / (4\pi\epsilon_o)^2 \hbar^3$ and $r_h = U_{Ar}/U_h$, U_h and U_{Ar} are the ionization potentials of hydrogen and argon, correspondingly; $P_{Bound}(t) = \epsilon_o \chi^{(3)}(1 - \rho(t)/\rho_{at})E(t)^3 + \chi^{+(3)}(\rho(t)/\rho_{at})E(t)^3 + \chi^{(5)}(1 - \rho(t)/\rho_{at})E(t)^5$, ϵ_o is the vacuum permittivity; m_e and q being the electron mass and charge, respectively; $\chi^{(3)}$ and $\chi^{(5)}$ are third and fifth order susceptibilities of neutral gas, correspondingly, while $\chi^{+(3)}$ is that of ionized gas. In the following we consider nearly collimated beams with diameter corresponding to a Rayleigh length larger than the propagation lengths. In addition, for these parameters the pump power is below the self-focusing power. Therefore, we can neglect diffraction in the numerical model. The transverse macroscopic plasma current $J_e(t)$ is determined by [19]:

$$\partial_t J_e(t) + v_e J_e(t) = \frac{q^2}{m_e} E(t) \rho(t) \quad (3)$$

where v_e is the electron collision rate (for argon $v_e \approx 5.7 \text{ ps}^{-1}$). Finally, the ionization energy loss is determined by $J_{Loss}(t) = W_{ST}(t)(\rho_{at} - \rho(t))U_{Ar}/E(t)$. A critical condition for an efficient frequency transfer to harmonics is the realization of phasematching which for intensities larger than the ionization threshold is sensitively influenced by the plasma contribution to the refraction index. The change of the linear refractive index of argon at the maximum of the pulse intensity I' (assuming Gaussian pulse shape), owing to the formation of laser plasma with a free electron density ρ' and the Kerr nonlinearity, is given by (see e.g., [28, 29]):

$$n(\omega, I', \rho') = n_e(\omega, \rho') + \Delta n_{Kerr}(I', \rho') + \Delta n_{Plasma}(\omega, \rho') \quad (4)$$

where $n_e(\omega, \rho') = (n^o(\omega) - 1)(1 - \rho'/\rho_{at}) + 1$, $\Delta n_{Kerr}(I', \rho') = I'[n_2(1 - \rho'/\rho_{at}) + n_2^+ \rho' + I' n_4(1 - \rho'/\rho_{at})]$ and $\Delta n_{Plasma}(\omega, \rho') = -q^2 \rho' / (2\epsilon_o m_e \omega^2)$.

The nonlinear susceptibility $\chi^{(3)}$ for argon is well known from many independent measurements, while only few experimental results exist for the higher-order susceptibilities. In [31,32] coincident experimental data on $\chi^{(5)}$ for argon which also agrees (up to sign) with a theoretical estimation [30] can be found. On the other hand reported data for $\chi^{(7)}$ differ by orders of magnitudes. Correspondingly, neglecting the weak frequency dependence we assume in the following parameters $\chi^{(3)} = 3.8 \times 10^{-26} \text{ m}^2/\text{V}^2$ and $\chi^{(5)} = -2.02 \times 10^{-47} \text{ m}^4/\text{V}^4$.

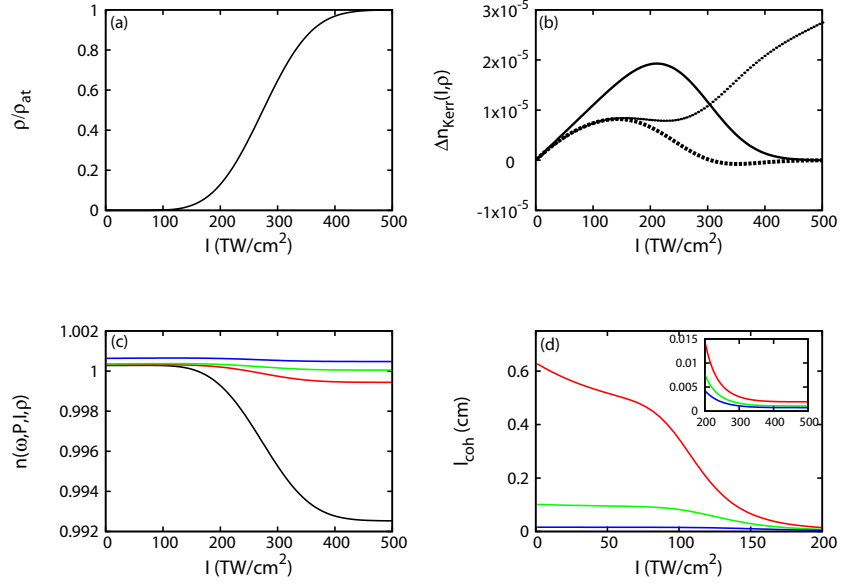


Fig. 1. Linear and nonlinear optical parameters of argon in the high-intensity regime (normal pressure $P = 1 \text{ atm}$) for a 20 fs pulse at 800 nm: (a) free electrons density at the trailing edge of the pulse normalized by the total number of atoms ($2.7 \times 10^{25} \text{ m}^{-3}$); (b) contributions of the nonlinear refractive index, caused by Kerr nonlinearity, when only $n_2 = 1.1 \times 10^{-23} \text{ m}^2/\text{W}$ (solid), n_2 and $n_4 = -0.36 \times 10^{-41} \text{ m}^4/\text{W}^2$ [31] (dashed), n_2 , n_4 and ionized argon $n_2^+ = 0.6 \times 10^{-23} \text{ m}^2/\text{W}$ [12] (dotted) are taken into account; (c) change of the total refractive index of pump (black), third (red), fifth (green) and seventh (blue), harmonics; (d) change of coherent length of third (red), fifth (green) and seventh (blue) harmonics.

Figure 1 shows some linear and nonlinear optical parameters of argon, calculated by using Eq. (4) for a 20 fs (FWHM) pump pulse at 800 nm in dependence on the pump intensity. Figure 1(a) shows the normalized plasma density after the pulse as a function of the pump intensity at the peak of the pulse. As can be seen full ionization at the trailing edge of the pulse occurs at around $450 \text{ TW}/\text{cm}^2$. Figure 1(b) shows changes of the Kerr-type nonlinear refractive index contribution $\Delta n_{\text{Kerr}}(I, \rho)$ taking into account (i) only n_2 of neutral argon (solid curve), (ii) n_2 and n_4 of neutral argon (dashed line) and (iii) n_2 , n_4 and n_2^+ of neutral and ionized argon (dotted line). Figure 1(c) shows the change of the refractive indexes of the fundamental frequency (black), third (red), fifth (green) and seventh (blue) harmonics. As can be seen the refractive indexes of the fundamental frequency and third harmonic are decreased down to a value smaller than unity. For higher intensities, the difference between the refractive indexes of the fundamental and the harmonics becomes larger, i.e., the generation of plasma electrons decreases the phase-matching length. This can be seen in Fig. 1(d) demonstrating the change of the coherent lengths ($l_{\text{coh}} = \pi/|\Delta k_{2r+1}|$) for different harmonics in dependence on the pump intensity. Here the coherent length strongly decreases above $100 \text{ TW}/\text{cm}^2$ for all harmonics.

Below we show that this behavior appears also in our full numerical calculations of Eqs. (1)-(3).

Neglecting bound electron contributions and the dependence of the pump intensity and plasma density on the propagation coordinate an analytical solution for the electric field of the harmonic has been derived in [14]. If we include the bound-electron contributions, the electric field for the harmonics with order of $2r + 1$ can be expressed as:

$$E_{2r+1}(z) = \sqrt{A_p^2 + \delta_{1r}(A_3 + A_{51})^2 + \delta_{2r}A_{52}^2} \sin(\Delta k_{2r+1}z/2) / (\Delta k_{2r+1}/2) \quad (5)$$

here $A_p = -\Phi k_o / (8\pi r(2r + 1)) (\omega_{pg} / \omega_o)^2 [\exp(-3r^2/\xi) + r/(r + 1) \exp(-3(r + 1)^2/\xi)] E_o$, $A_3 = 3\mu_o c \epsilon_o \chi^{(3)} E_o^3 \omega_o / 8$, $A_{51} = 15\mu_o c \epsilon_o \chi^{(5)} E_o^5 \omega_o / 2$, $A_{52} = 5\mu_o c \epsilon_o \chi^{(5)} E_o^5 \omega_o / 32$; δ_{ij} is Kronecker's symbol; $\omega_{pg} = 4\pi\rho_{at}q^2/m_e^2$ is the plasma frequency associated with the initial gas density; $\Phi = 8\sqrt{3}\pi(\omega_a/\omega_o)\xi^{1/2}\exp(-2\xi/3)$, $\xi = E_a/E_o$, E_o , ω_o and k_o are peak electric field, central angular frequency and wavenumber of pump, respectively; Δk_{2r+1} is wave mismatch for $(2r + 1)^{th}$ harmonic. The term A_{51} describes the contribution of fifth-order susceptibility $\chi^{(5)}$ to the generation of third harmonic. We note that the relative phase of the fields generated by bound-electrons and the plasma current is $\pi/2$. In the following we compare this solution with the numerical solutions of the full model as presented in Eqs. (1)-(3).

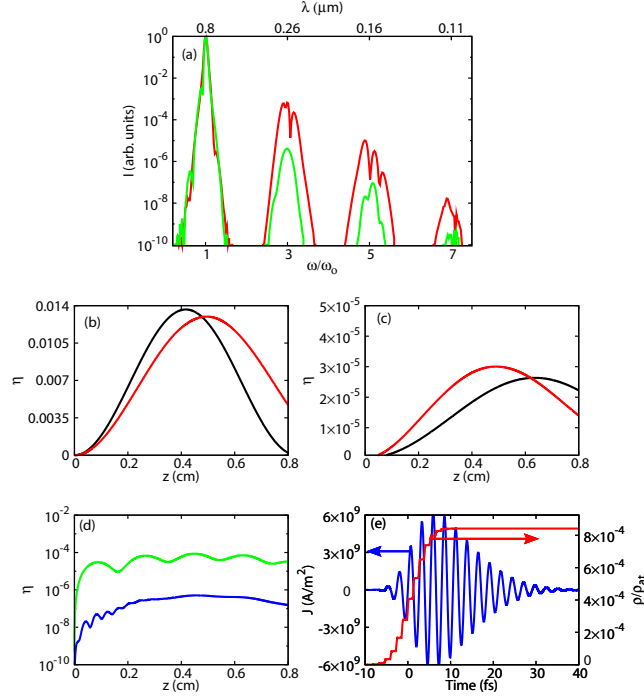


Fig. 2. Numerical and analytical calculations for a 20-fs transform limited pump pulse with a 100 TW/cm^2 peak intensity at 800 nm: (a) spectrum of the output pulse, calculated numerically with (red) and without (green) taking $\chi^{(3)}$ and $\chi^{(5)}$ into account; (b) efficiency conversion of third harmonic, calculated numerically (red) and analytically (black) for $\chi^{(3)} \neq 0$, $\chi^{(5)} \neq 0$, and $\chi^{(3)} = \chi^{(5)} = 0$ (c); (d) efficiency conversion of fifth (green) and seventh (blue) harmonics; (e) normalized free electron density in time domain (red) and plasma current (blue).

3. Numerical results for 800-nm pump

In this chapter we present numerical solutions of Eqs. (1) to (3) using the split-step method with fast Fourier transformation and the fifth-order Runge-Kutta method for 800-nm pump pulses with a 100 TW/cm^2 peak intensity and 20-fs (FWHM) duration.

The spectra in Fig. 2(a) calculated with (red) and without (green) contribution of $\chi^{(3)}$ and $\chi^{(5)}$ predict that LOHG is dominated by the bound electron contributions with the third and fifth order susceptibilities, since with $\chi^{(3)} = 0$ and $\chi^{(5)} = 0$ two order of magnitude lower efficiencies are predicted. In Fig. 2(b) and 2(c) analytical (black) and numerical (red) results for the efficiency of third harmonic conversion are compared for cases, when $\chi^{(3)} \neq 0$ and $\chi^{(5)} \neq 0$ (b) is included and for $\chi^{(3)} = \chi^{(5)} = 0$ (c). Note that we calculated the efficiency by integration of the harmonic spectra.

The analytical results are calculated by Eq. (5), using the wave vector mismatch with a constant pump intensity and a plasma density taken from the input parameters. These results confirm the conclusions drawn from Fig. 2(a) that at the optimum intensity of about 100 W/cm^2 the bound-electron contribution is much larger than that of the tunnel ionization current. It should be noted that the maximum efficiency of the third harmonic of about 1.4 % appears at 0.4 cm, which is approximately equal to the coherent length, as seen from Fig. 1(d). Figure 2(d) shows the efficiency of conversions to the fifth (green) and seventh (blue) harmonics with maximum values of about 10^{-4} and 10^{-7} . In Fig. 2(e) the normalized plasma current and the plasma density are presented. Note the steplike nature of the density profile of free electrons (red curve), which explains the source of the harmonic generation due to the tunnel ionization current.

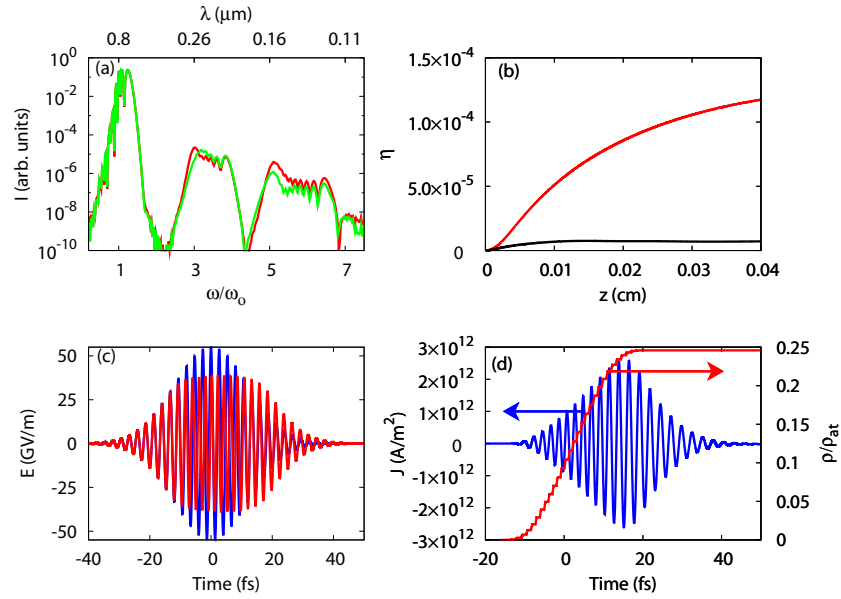


Fig. 3. Numerical calculations for a 20-fs transform limited pump pulse with 400 TW/cm^2 peak intensity at 800 nm: (a) spectrum of the output pulse, calculated with (red) and without (green) taking $\chi^{(3)}$ and $\chi^{(5)}$ into account; (b) conversion efficiencies of third (red) and fifth harmonics (black); (c) time profile of the pump at the input (blue) and output (red); (d) normalized density of free electron distribution (red) and plasma current (blue).

To study the regime where the tunnel-ionization current is dominant, in Fig. 3 results for LOHG are presented for a 20 fs pulse at 800 nm with an peak intensity of 400 TW/cm^2 . Due to

the reduced coherence length the maximum conversion efficiencies are smaller than for the case of lower pump intensity in Fig. 2. Since the efficiencies are roughly the same independent on the inclusion of $\chi^{(3)}$ and $\chi^{(5)}$ in the model, we can conclude that the tunnel-ionization current is the main LOHG mechanism in this case.

Due to the high intensity significant spectral broadening caused by self-phase modulation can be seen. The dependence of the efficiencies on the propagation distance indicates pump depletion rather than loss of coherence, since it exhibits no maximum. Here pump depletion, owing to ionization loss, appears mainly in the pulse center, as shown in Fig. 3(c).

In order to analyze the roles of the $\chi^{(3)}$, $\chi^{(5)}$ and $\chi^{+(3)}$ nonlinearity and the tunnel-ionization current in dependence on the applied intensity range, we calculated the contribution to LOHG efficiencies of the two considered nonlinear optical processes in a large range of pump intensities. Figure 4 shows the conversion efficiencies in dependence on the pump intensity up to the 7th harmonic from a 800-nm pump with a 20-fs duration, calculated at the coherent length of third harmonic. The contribution of $\chi^{(3)}$ and $\chi^{(5)}$ dominates up to 300 TW/cm², while after approximately 300 TW/cm² the plasma current (red curves) becomes the main source for LOHG. The green curve in Fig. 4(a) shows results, which includes $\chi^{+(3)}$ of the ionized gas. For high intensities up to 500 TW/cm² the efficiency of THG decreases down to the range of 10⁻⁵.

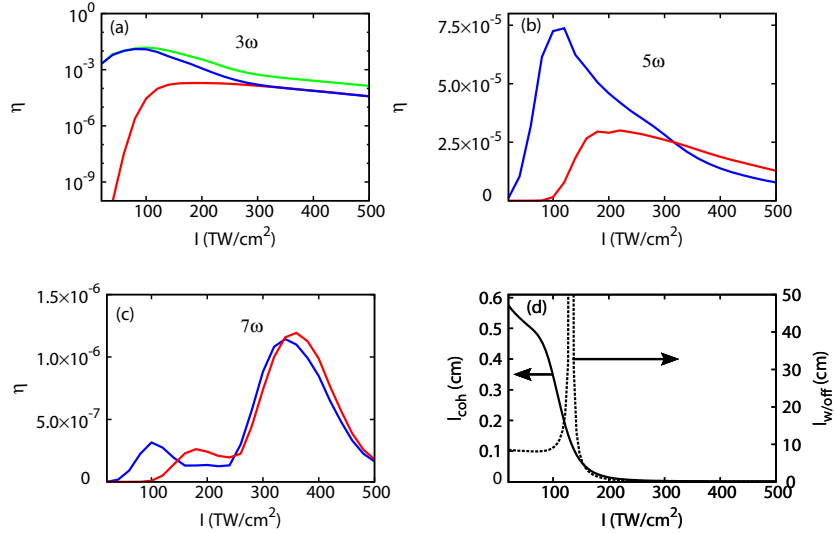


Fig. 4. Efficiency of LOHG in dependence on the pump intensity calculated for (a) third, (b) fifth and (c) seventh harmonic. Efficiencies were calculated with (blue) and without (red) taking $\chi^{(3)}$ and $\chi^{(5)}$ into account. Green curve in (a) shows results when $\chi^{(3)}$, $\chi^{(5)}$ and $\chi^{+(3)}$ were taken into account. In (d) the change of the coherent length of third harmonic and the length of its temporal walk-off from the fundamental frequency are shown.

It seems to be surprising that even for relatively high intensities from 150 to 300 TW/cm² the contribution of the $\chi^{(3)}$ and $\chi^{(5)}$ process remains in the same order as that of the tunnel-ionization current. This can be explained by the fact, that full ionization only occurs at the trailing edge of the pulses, while at the leading edge the atoms are not ionized and bound-electron contributions still play a significant role. The length of temporal walk-off between the fundamental and the third harmonic is shown in Fig. 4(d). It is much larger than the coherent lengths, and therefore does not play a significant role during propagation.

A general observation arising from the results presented above is that the nonlinear susceptibilities $\chi^{(3)}$ and $\chi^{(5)}$ plays an important role in the formation of LOHG, especially for the

third harmonic. Its contribution is dominant up to a pump intensity of 300 TW/cm^2 for argon at normal pressure. As similar behavior can be expected for other noble gases, although the corresponding intensities will vary dependent on the properties of the noble gas. The tunnel-ionization current is a main source for LOHG for intensities larger than approximately 300 TW/cm^2 , especially for the fifth and seventh harmonics. As noted above, the high-intensity regime of pump can not support highly efficient LOHG because of the the contribution of the ionized electrons to the refraction index and the associated increased phase mismatch. Below 100 TW/cm^2 , the coherent length is roughly constant, but for larger intensities it shows a sharp decrease as visible in Fig. 1(d) and Fig. 4(d). This establishes a range around 100 TW/cm^2 as optimum pump intensity for argon for the generation of the third and fifth harmonic.

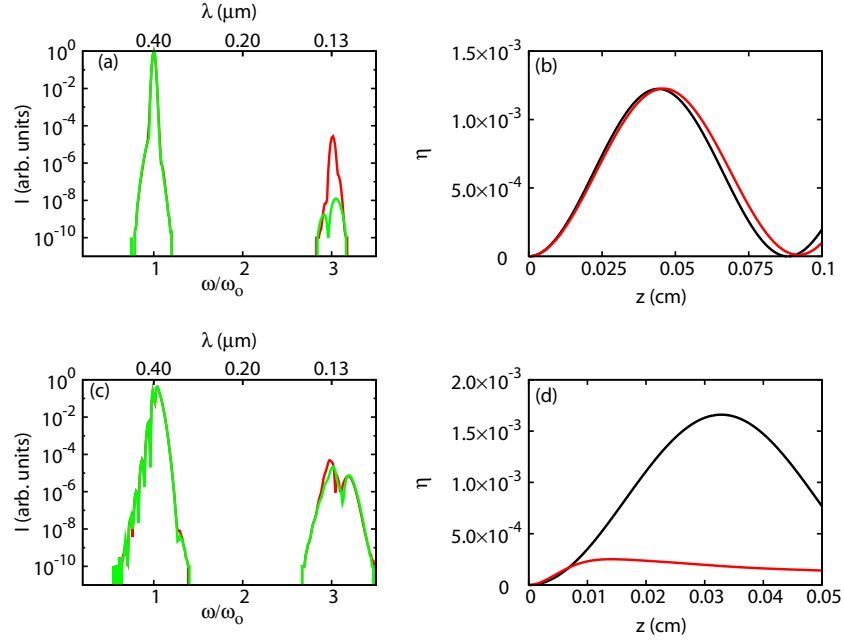


Fig. 5. Results of numerical and analytical calculations for 400 nm pump pulses with 100 TW/cm^2 [(a),(b)] and 300 TW/cm^2 [(c), (d)]. In (a), (c) the spectrum of the output pulses, calculated with (red) and without (green) taking $\chi^{(3)}$ and $\chi^{(5)}$ are presented. In (b), (d) the efficiency of third harmonic, calculated numerically (red) and analytically (black) are shown.

4. Numerical results for 400-nm pump

Nowadays, the generation of pump pulses at 400 nm with high energy by second harmonic generation in nonlinear crystals from near-IR ones is a standard method. Using THG with these pump pulses allows frequency conversion with relative high efficiency into the VUV spectral range at 133 nm. Figure 5 shows the results for such pump pulses with two different peak intensities for 100 TW/cm^2 (a, b) and for 300 TW/cm^2 (c, d) and the same pulse duration of 20 fs. The coherent length for the third harmonic is around a 0.05 cm (0.024) cm for 100 (300) TW/cm^2 , calculated by Eq. (4) and visible in Fig. 5(b) and 5(d). The tendency visible from Figs. 2 and 3 that for a lower intensity THG is caused by the third and fifth order susceptibilities while for higher intensities the tunnel ionization current plays the dominant role, is also observed for 400 nm as can be seen by comparison of Fig. 5(a) and 5(c). The maximum THG efficiency of

about 1.5×10^{-3} for a pump intensity of 100 TW/cm^2 [Fig. 4(b)] is in the same range as in the case of a 800 nm pump pulses compare [Fig. 2(b)], but now a spectral transformation to the VUV range at 133 nm is realized. Higher harmonic orders above third, experience high linear loss of in the vacuum ultraviolet region for argon [33] due to the strong absorption band below 106 nm.

5. Conclusions

In conclusion, we numerically studied the generation of low-order harmonics in argon in the high-intensity regime, when tunneling ionization takes place. The used numerical method is based on the unidirectional pulse propagation equation combined with the nonlinear response by the bound-electrons and a model for tunneling ionization and the associated plasma current. We analyzed LOHG in the regime of pump intensities up to 500 TW/cm^2 arising either from the third- and fifth-order bound-electron nonlinearity or from the tunnel-ionization current. It was numerically observed that up to 300 TW/cm^2 the formation of LOHG is caused mainly by the bound-electron nonlinearity, while for higher intensities the tunnel-ionization current plays the dominant role. It was also shown that a high intensity of the pump does not necessary lead to efficient LOHG, rather, due to the reduced coherence length by the plasma contribution to the refraction index an optimum around 100 TW/cm^2 with efficiencies in the range of 3×10^{-3} and 10^{-4} for third and fifth harmonic generation, respectively, is predicted. Further on, we studied THG by intense pump pulses at 400 nm and predicted frequency transformation to the spectral range of 133 nm with maximum efficiency of about 1.5×10^{-3} .

Acknowledgments

We acknowledge financial support by the German Research Foundation (DFG), project No. He 2083/17 – 1.